iJRASET
International Journal For Research in Applied Science and Engineering Technology

INTERNATIONAL JOURNAL FOR RESEARCH

IN APPLIED SCIENCE & ENGINEERING TECHNOLOGY

Volume: 7 **Issue:** XI **Month of publication:** November 2019

DOI: http://doi.org/10.22214/ijraset.2019.11006

www.ijraset.com

Call: 08813907089 | E-mail ID: ijraset@gmail.com

International Journal for Research in Applied Science & Engineering Technology (IJRASET)
ISSN: 2321-9653; IC Value: 45.98; SJ Impact Factor: 7.177
Volume 7 Issue XI, Nov 2019- Available at www.ijraset.com

Analysis of a Parallel Manipulator Implemented in Four-Dimensional Radiotherapy for Physiological Motion of Human Tissues

Darmakari Ravi Abhinay Kumar[1], Dr. G. Satish Babu[2]
[1]*M-Tech student,* [2]*Professor, Department of Mechanical Engineering, JNTUH College of Engineering, Hyderabad*

Abstract: ***Radiotherapy (RT) permits a selective destruction of cancer cells, although the treatment region is constrained to the irradiated region. Any radiation method comes along side a couple of sources of errors that may result in a deviation of the dose that is implemented to the affected man or woman. Phantoms—systems that reflect a human and consist of measurement technology to assess the implemented dosage are used to make such mistakes identifiable. Past RT technology applied to non moving or stationary tumours. Correspondingly, most current phantoms contain static components. Nowadays, RT is at a transition stage towards strategies which explicitly account for organs which displace all through surgery. These techniques require phantoms generating such movement. Consequentially, a demand for new types of manipulators, which function with a RT-phantom, has stand up and could further increase within no time. Key demands of such manipulators are amongst others, the technology of whole inflexible body motion, immoderate acceleration, high stiffness, compactness, little weight, and easy portability.In this report, a modern kind of parallel kinematic manipulator (PKM), which is tailored to the necessities of 4-Dimensional RT-phantom era, is obtainable. The PKM consists of low price standardized mechanical constituents and units the intention structures, which can be positioned inner a human-equivalent location, into translational and rotational motion in 3 degreess-of-freedom (DOFs). Only a part of the end-effector is located inside the human-equivalent region.Two versions of the manipulator are provided in the report: their kinematics are derived and their kinetostatic properties are also compared. This includes a workspace analysis and the analysis of the transmission behaviour for the required movement, which means the influence of the maximum critical layout parameters at the overall performance. It may be shown that realistic differences of both kinematics are negligible, while the modified model offers significant mechanical advantages. In end, a first special reason manipulator for application inside the evolving field of RT-phantom era is offered. The PKM, which employs a novel kinematic shape, presents better suitability for its reason than most of the other robotic systems to this point for the same motive.***
Keywords: Degree of freedom, Parallelrobot, kinematicanalysis, inversekinematics, workspace analysis.

I. INTRODUCTION

Radiotherapy, chemotherapy and Surgery are the 3 foremost ways of destroying cancer tissues. Analogous to chemotherapy, radiotherapy (RT) permits a selective destruction of tumour cells. With radiotherapy, the treatment location is confined to the irradiated location, as a result averting a systemic damage to the affected person.

Evolution of RT goals at increasingly more centered irradiation of the tumour at the same time as increasingly sparing surrounding healthful tissue, mainly organs at risk including the spinal cord, heart, or brachial plexus.

Modern RT strategies like depth modulated radiotherapy allow dose application with excessive spatial precision and accordingly effective remedy of stationary tumours. Four-dimensional RT techniques (4D-RT) mark a new technology of RT and are an increasing number of addressed in both studies and scientific routine. These techniques provide a real-time adaption of the radiation cognizance to temporal modifications of the tumour and its environment. Thus, the irradiation concentration may be confined to the tumour despite the fact that that tumour performs significant physiological motion, e.g., as a result of respiration.

Radiotherapy comes at the facet of a couple of probability of mistakes that could enhance a fluctuation in the dose this is carried out to the affected person. Such errors might also additionally result in effecting a healthy tissue which is near to the affected tissue, e.g., from deviation of predetermined dose distribution within the affected organ. Phantoms are used to make such mistakes observable.

A phantom offers a human-same shape, i.e., its structural components effectuate the dose absorbance traits of a human body. In addition, a phantom gives measurement generation to evaluate the dosage accomplished to the phantom.

Phantoms are required for studies, development, and scientific validation of latest RT techniques. Also, phantoms are completed regularly for the non-prevent quality assurance (QA) of those techniques in scientific workout. They are used to verify, analyze, and

accurate the executed RT way internal a remedy setting such that increases predictability, protection, and robustness of the method can be ensured. Also, for each inversely generated RT plan, kinematic parameters can be effectively tested throug the use of a phantom in advance than an affected man or woman is treated. In future, the dosimetric accuracy required for advanced RT strategies will growth in addition, mainly pushed throug the use of the continued evolution of scientific imaging techniques, which permit more and more precise localization of tumour and hazard structures.

II. ROBOT DESIGN

The epic automated format dependent on a parallel kinematic shape is portrayed in figure Furthermore, the kinematic shape is demonstrated in figure The mechanical sets the objective (T) into adjustable relative development with acknowledges to the edge (B). The objective reproduces the moving tissue frameworks of an influenced individual, e.g.,the tumor and healthy abutting tissue. The body (B) encompasses the objective and imitates the non moving tissue frameworks of a patient, e.g.,the thorax with ribs, lungs, and spine.

Along these lines, target and body speak to the human-tissue-comparable and dosimetric added substances of the 4D-apparition, while the automated contains the mechanical and mechatronic added substances to set objective and edge into relative development. The robot incorporates a parallel kinematic structure. The end effector (E) of the automated is inflexibly connected to the objective.

The body (0) of the automated is inflexibly connected to the body just as, alternatively, to the patient work area. All the refered to associations can be easily made separable and precisely restorable to deftly connect extraordinary our bodies and targets with the automated and to deftly fix the 4D-ghost on selective patient tables in accordance with the logical interest.

Three same appendages (dynamic steerage) join the endeffector to the body. Every appendage comprises of a shaft screw (S) driven by utilizing a stage engine which is associated with the body through a general joint (U). The screw nut (N) is appended to the end-effector by means of an ordinary joint (U) as pleasantly. The pivot of the progression engine executes a necessary separation between the 2 previously mentioned all inclusive joints. Moving the center of turn of the stop effector and contorting of the end-effector about the longitudinal hub are deflected with the guide of an additional inactive direction: The quit-effector slides through a kaleidoscopic joint (P), whose direction (G) is connected to the body by method for revolute joints which structure a normal joint. The tomahawks of revolution meet on the focal point of the direction.

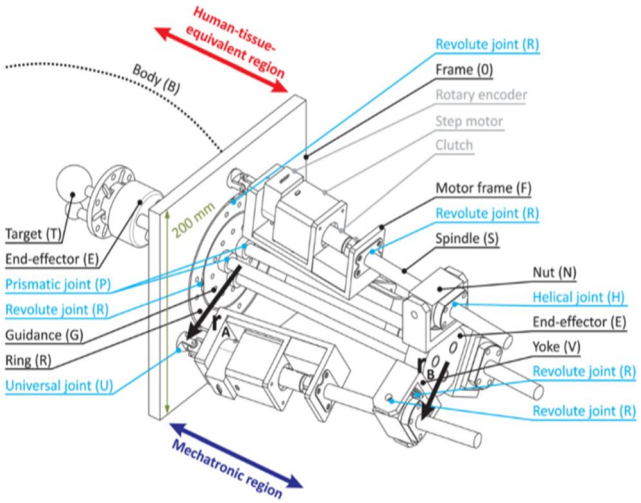

Fig.1. The robot and its main mechanical components (base version).

So as to improve design, assembling, and meeting of the mechanical, an open door kinematic shape has been progressed. This shape moves the counter winding quality of the detached directing to one of the appendages. Thusly, 1DOF (revolute joint) of one famous joint at the stop effector is evacuated, following in an unbending association among one burden and the end-effector.

What's more, the kaleidoscopic joint can be supplanted by a barrel shaped joint, and the state of the stop-effector might be disentangled to one single bar with raised breadth, that is essentially helpful concerning the prerequisites of a steel-free and hardened quit-effector and for the aversion of bracing results, which may emerge between stop effector and steerage. Along these lines, the mechanical intricacy of the robot is comparably diminished and its firmness might be extended.The robot has been tailored to the specific demands of 4D-phantoms and 4D-RT, presenting the subsequent functions:

1) On the main hand, the objective can be moved translational and rotationally. The ordered arrangement of the directions might be picked openly and balanced , with the goal that convoluted movements of the objective are suitable.

2) On the other hand, best some portion of the endeffector is situated inside the human-tissue-identical locale. All the inverse mechatronic parts of the robot are spatially isolated from that region. Tissue comparability over the whole volume of the casing is in this manner created through the exact texture determination of the surrender effector.

3) Furthermore, the parallel kinematic structure of the mechanical permits inordinate increasing speeds and has a little working space. Another wellknown increase of parallel kinematic frameworks in evaluation to sequential inverse numbers is the extreme solidness, and accordingly the inordinate situating exactness .

4) The robot has just some institutionalized mechanical parts, that are vigorously structured and avoid change or mechanical harm of the robot even underneath hard logical conditions.

5) The symmetrical direction of the body concerning the surrender effector ermits level fathoming of casing and aspect mass of the edge. This diminishes the multifaceted nature of a nflexible and explicit mechanical association among body and robot.

6) Moreover, the in a flash lined pipe-formed endeffector gives a simple access channel to the objective, which rearranges inclusion of fastened size gadgets (e.g., onization chambers). Likewise, extra development delivering actuators is presumably applied on the objective through this channel .

III. KINEMATIC MODELLING

The kinematic structure of the PKM is portrayed in figure The latent directing and each dynamic appendage are connected in a steady progression with body and end-effector. As indicated by the gathering of kinematic chains , the system can be described as a 3URHU-1UP mechanical. This kinematic structure is close to the 3UPS-1UP structure of the Tricept. A noteworthy highlights, which recognize the kinematic structure of the 4D-ghost from that of the Tricept, are as per the following: Manipulation on one side and incitation (automated) on the opposite side of the body and Structural against curve controlling among engine and screw nuts, that is performed with the guide of the utilization of two normal joints as heading of every appendage.

Some notations have been used in the following figures to understand various components of the manipulator as explained below.

B: body	N1-3: nut
O: frame/base	U: universal joint
G: guidance	C: cylindrical joint
E: end effector	R: revolute joint(passive)
T: target	*R*: revolute joint (active)
F1-3: motor frame	H: helical joint
S1-3: spindle	P: prismatic joint

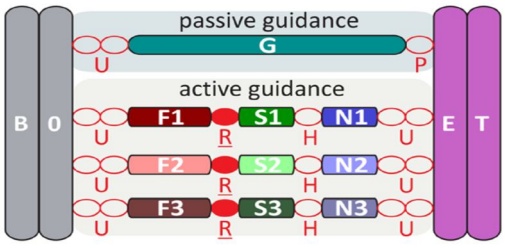

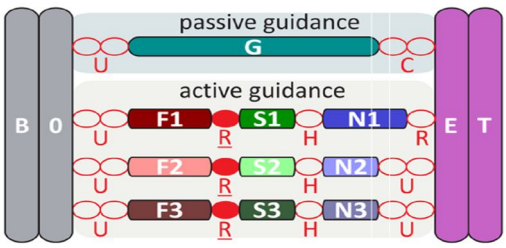

Fig.2. Kinematic structure of the robot (base version). Fig.3. Kinematic structure of the robot (modified version).

The last element lessens the mechanical multifaceted nature of the entire structure however effectuates a posture subordinate certain auxiliary turn between each screw and nut, which should be incorporated into the kinematic portrayal. Likewise, erosion torques of each screw are transmitted to the end-effector, along these lines expanding its solidness prerequisites. The mechanical structure without the direction is by all accounts like a 3UPU structure, yet the internal all inclusive joint tomahawks (appendage side widespread joint tomahawks) are not parallel to one another, so the depicted structure has two rotational DOFs as opposed to the 3UPU structure with three translational DOFs. Circular robots, for instance, give a few rotational DOFs however show a complex and hence cost serious mechanical get together. Likewise, the rotate purpose of the end-effector can't be bolstered by a mechanical direction (as this would overconstrain the framework), which significantly diminishes the robot solidness. The modified rendition of the 4D-apparition can be portrayed as a 2URHU-1URHR-1UC structure .

ISSN: 2321-9653; IC Value: 45.98; SJ Impact Factor: 7.177
Volume 7 Issue XI, Nov 2019- Available at www.ijraset.com

A. Reference Frames And Notation

The reference outlines, which are required for processing the changes of robot arranges, are clarified further. In this work, vectors are spoken to in segment structure as it were.A position column vector is denoted by r with three indices appended

- Upper left-hand side index: Denotes the coordinate system in which the vector components are expressed.
- Lower left-hand side index: Denotes the starting point of the vector.
- Lower right-hand side index: Denotes the end point of the vector.
- Rotational matrices are denoted by R, with two indices appended defining argument and result of the product between R and a position column vector.
- Lower right-hand side index: Denotes the coordinate system in which the components of the argument position column vector are expressed.
- Upper left-hand side index: Denotes the coordinate system in which the components of the resultant position column vector are expressed.

In light of the previously mentioned record show, the accompanying holds:

$$^{K}_{m}r_{n} = {}^{k}R_{p}\ {}^{p}_{m}r_{n} \qquad (1)$$

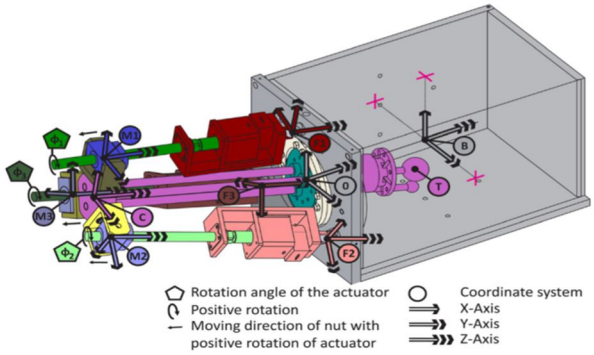

Fig.4. Reference frames of the phantom robot.

A file, which is overlooked, shows the base outline, which is indicated as "0." The grids Rx, Ry, and Rz mean the rudimentary turn frameworks for pivot about the x, y, and z-directions, separately. Contentions of capacities and calculations are shown in wavy sections

Opposite Kinematics. The forward kinematics of an all inclusive joint, which actualizes a first revolution about the x-hub with point Øx and a second pivot about the y direction with edge Øy, can be portrayed as

$$^{1}d_{z2} = R_{x}\{\ Ø_{x}\ \}\ R_{y}\{\ Ø_{y}\ \}^{2}\ d_{z2} \qquad (2)$$

where the previously mentioned pivots reorient framework 1 to framework 2, and 1dz2 and 2dz2 speak to a vector of length d, which is arranged along the z-hub of framework 2. The reverse kinematics of an all inclusive joint can be found by reversal of Eq. (2) a

$$Ø_{x} = \tan^{-1}\{{}^{1}d_{z2(y)}/{}^{1}d_{z2(z)}\}\ ;\ Ø_{y} = \tan^{-1}\{{}^{1}d_{z2(x)}/d\}$$
$$^{1}R_{2} = R_{x}\{\ Ø_{x}\ \}\ R_{y}\{\ Ø_{y}\ \} \qquad (3)$$

where 1dz2(x), 1dz2(y),and 1dz2(z), denote the x, y, and z components of vector 1dz2. In the following, implementation of Eq. (3) is indicated by the symbol U{ }, e.g., {1R2, Øx , Øy } = U{1dz2 }, where 1dz2 is the input vector, and 1R2, Øx and Øy are the used output quantities of the mathematical calculations. The end-effector coordinates are denoted as c = [Ø1 Ø2 l]T

Alluding to the documentation delineated in Figure the end-effector directions can be gotten from the situation of the objective BBrT as

$$l = |r_{B} + R_{B}\ {}^{B}_{B}r_{T}|$$
$$\{R_{G}, Ø_{1}, Ø_{2}\} = U\{r_{T}\} \qquad (4)$$

Base Version. Alluding to the documentation delineated in Figure, the change of the end-effector facilitates c into the engine points $\theta = [\theta_{(1)}\ \theta_{(2)}\ \theta_{(3)}]^{T}$ for the base version of the robot is given by the following algorithm:

1) Direction of the inactive direction (G)

$$R_G = R_x\{ Ø_1 \} R_y\{ Ø_2 \} \quad (5)$$

2) Position of framework

$$Cr_C = (l-l_C) R_G e_z \quad (6)$$

where l_C and e_z denote the length of the end-effector and the elementary unit vector in z-direction, respectively

3) Direction of framework C

$$R_c = R_G \quad (7)$$

4) Places of frameworks M1, M2, and M3

$$r_{Mi} = r_c + R_c {}^{c}r_{Mi} \quad i \in [1,2,3] \quad (8)$$

5) Separations Between Frameworks F1, F2, and F3 and M1, M2, and M3, Individually,

$$_{Ni}rFi = r_{Fi} - r_{Ni} \quad i \in [1,2,3]$$
$$l_{(i)} = |_{Ni}rFi| \quad i \in [1,2,3] \quad (9)$$

6) Directions of Frameworks F1, F2, and F3

$$\{ {}^{Fi0}R_{Fi} \} = U\{ R^{T}_{Fi0\ Ni}rFi \} \ i \in [1,2,3]$$
$$R_{Fi} = R_{Fi0}\ {}^{Fi0}R_{Fi} \quad i \in [1,2,3] \quad (10)$$

7) Directions of Frameworks M1, M2, and M3

$$\{ {}^{Ni0}R_{Ni} \} = U\{ (R_C {}^{C}R_{Ni0})^{T}\ _{Ni}rFi \} \ i \in [1,2,3]$$
$$R_{Ni} = R_C {}^{C}R_{Ni0}\ {}^{Ni0}R_{Ni} \quad i \in [1,2,3] \quad (11)$$

where M10, M20, and M30 signify the edges M1, M2, and M3 for the instance of zero turns of the related widespread joints.

8) Edges of (basic) turns of frameworks M1, M2, and M3 as for frameworks F1, F2, and F3.

$$\hat{\theta}_{(k)} = \tan^{-1}\{ (R_{Fk}e_y)^{T} (R_{Nk}e_y) / (R_{Fk}e_y)^{T} (R_{Nk}e_x) \} \quad k \in [1,2,3] \quad (12)$$

where ex and ey indicate the rudimentary unit vectors in the x and y headings, individually.

9) Engine edges

$$\theta(i) = (l_{(i)} - l_{0(i)})2\pi / \mu - \hat{\theta}_{(i)} \quad i \in [1,2,3] \quad (13)$$

where l means the pitch of the string, and l0(1) , l0(2) and l0(3) indicate the separations between F1, F2, and F3 and M1, M2, and M3 at zero engine points θ (1) , θ (2) and θ (3) separately.

Adjusted Version, For the modified robot adaptation, just the computation of the direction of framework C changes to Orientation of framework C.

$$e_{zC} = -r_C / |r_C|$$
$$e_{yC} = r_{F1} \times r_C / |r_{F1} \times r_C|$$
$$e_{xC} = e_{yC} \times e_{zC}$$
$$R_C = [e_{xC}\ \ e_{yC}\ \ e_{zC}] \quad (14)$$

B. Jacobian Matrix

The opposite kinematic calculation is differentiable for both the base and the modified variant of the robot. In this way, the Jacobian grid, defined as $J = [\partial\theta/\partial c]^{T}$, is found by expository separation of the backwards kinematic calculation as defined above.

C. Kinematic And Kinetostatic Analyses

So as to recognize the exhibition of the created 4Dphantom, a workspace examination pursued by a kinetostatic investigation including speed and power/torque transmission is performed. To do as such, the kinematic model and the estimation of the Jacobian framework are actualized in MATLAB®

D. Workspace analysis.

The workspace examination is executed so as to investigate the reachable workspace for the exhibited 4D-ghost. The reachable workspace portrays the workspace which contains all the reachable focuses by the TCP (point T, alluding to the documentation delineated in Figure). For this situation, the TCP is situated at the focal point of the objective. Volume and shape are two criteria to depict and assess the properties of the reachable workspace. A further paradigm is the size of geometrical objects (e.g., solid shape, chamber, and circle) that can be encased by the reachable workspace. Since the reverse kinematics issue is scientifically resolvable for this PKM, legitimate workspace focuses can be resolved

For Selected Configuration. figure shows the reachable workspace of a chose parameter configuration (nitty gritty specifications in the following sections) of the 4D-ghost's TCP as a volume, the workspace limits as spots, and the biggest circle that fits into the workspace. The workspace is restricted by the negligible and maximal string lengths of the axle. A geometrical thought of the workspace (with dismissing the inward joint cutoff points) would bring about a bended cone-molded workspace.

The obtainable ws space is 1.5×10^{-3} m^3; the biggest ball has a space of 0.2×10^{-3} m^3. Hence, the volume covers 18% of the complete workspace volume. There is no discernible distinction between the base and the modified kinematic form as the two adaptations show just little contrasts in the hub pivot of the end-effector, whose effect on the workspace is insignificant.

For Other networks. So as to examine the workspace properties of the chose configuration in contrast with other conceivable parameter settings, a general workspace investigation is performed. Just two significant parameters are identified: the range of the hover shaped by the all inclusive joints that associate the appendages to the base casing, rA, and the sweep of the hover framed by the all inclusive joints that interface the appendages to the end-effector rB. Both plan parameters, rA and rB, are portrayed in figure The accompanying suppositions are made:

1) Variation of the casing span rA in a scope of 50–150mm, advance size 10mm,
2) Variation of the end-effector sweep rB in a scope of 20–120mm, advance size 10mm,
3) rB < rA, and
4) Thread length of the axles 150mm<s<240mm

For all parameter blends, the volume of the reachable workspace and of the biggest circle is determined. The outcomes are appeared in figures. The present parameter choice is set apart with a cross (rA = 80 mm and rB = 58.981 mm). The workspace volume increments with diminishing casing and end-effector sweep. Simultaneously, the volume of the biggest circle marginally increments, however it is maximal for an enormous edge range and a little end-effector span. The last configurations in this way show the best proportion of circle volume to workspace volume. For the application in a 4D-RT forms, the recommended workspace is a 3D shape with side lengths a = 45mm. On the off chance that the biggest circle inside the reachable workspace encases this 3D shape, workspace limits won't be surpassed. Along these lines, half of the block's inclining (0.5 dia) decides the base sweep rmin of the circle, which completely covers the 3D square, as indicated by the accompanying condition.

$$r_{minn} = \frac{d}{2} = \frac{\sqrt{3}\ (side)}{2} \approx 39\ mm \qquad (15)$$

As needs be, the base circle volume to be encased by the reachable workspace volume adds up to 0.248 ×10-3 m3. In figure, this point of confinement is set apart with a ran line. This implies all the parameter blends underneath this line agree to the necessities for the recommended workspace. Subsequently, the edge sweep can be expanded or diminished, while the end-effector span should just be decreased to broaden the volume of the biggest circle contrasted with the chose configuration. To assess the presentation of the robot for the underlying and other parameter mixes, a kinetostatic examination is performed.

E. Kinetostatic Analysis

In view of the opposite kinematics and the Jacobian lattice, a kinetostatic examination permits assessing the transmission conduct of the robot as to drive and yield amounts. For instance, this incorporates for a given burden case the accompanying assessment procedure:

1) Necessary drive torques,
2) Necessary actuator speeds, and
3) Required incitation control.

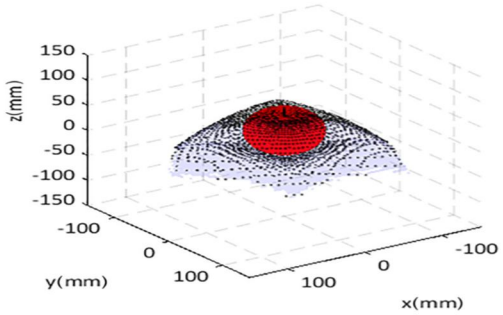

Fig.5. Workspace with enclosed largest sphere of the selected configuration.

The increasing velocities of connections and their idleness properties are not considered. For further computations, the accompanying commendable burden case is applied to the objective (point T, alluding to the documentation portrayed in figure):

$$f_T = [\ 5N \quad 5N \quad 20N]^T$$

$$\dot{r}_T = [\ 0.019 \quad 0.019 \quad 0.076\ ]^T$$

where fT is the power vector, and ṙT is the speed vector. It is accepted that a power of 20 N is applied to the objective in the z-heading. The body can be filled with various fluids that speak to the human body. The objective needs to move in this condition. Consequently, the applied burden case incorporates a high, speed subordinate, grating power that should fall underneath much of the time. The speed vector is gotten from the ideal movement of the objective. This movement can be portrayed with the accompanying vector as for the reference outline B of the body (Lujan model to reproduce breath developments)

$$^{B}{}_{B}r_T(t) = [\ 0 \quad 0 \quad -\hat{x}\cos(f\pi t)4\ ]^T \qquad (16)$$

The adequacy x is set to 10mm, and the recurrence f is 0.5 Hz. The limit of the first time-subordinate is the greatest happening speed. The speed/power vector of the end-effector (ṙT, fT) is identified with the actuator speed/torque vector (ω, τ) by the Jacobian lattice Jxyz, which is found by (logical) separation of the engine edges as for the translational objective situation as

$$J_{xyz} = [\partial\theta/\partial r_T]^{-1}.$$

The activation power can be determined for each point inside the endorsed workspace and for every actuator I.

The previously mentioned criteria (actuator torques, actuator speeds, and incitation control) are utilized to investigate the transmission conduct inside the endorsed workspace, i.e., a 3D shape with side length a=45mm and focus direct equivalent toward the focal point of the biggest circle. For each point inside the recommended workspace, just the greatest supreme worth (speed, power, and intensity) of one of the three actuators is considered. The outcomes are exhibited for the chose configuration in figure.

A further examination incorporates the figuring of the maximal estimations of various properties (e.g., actuator powers or speeds) inside the biggest, cubic workspace that fits into the biggest circle for every parameter mix (rA,rB). The outcomes are displayed in figures. Once more, the farthest point for a 3D shape with side length a=45mm is set apart by a ran line.

A cross shows the present configuration (base variant). By and large, the scope of the most extreme qualities is little. Particularly, if the middle qualities if the middle qualities (not appeared here) are considered, the properties are homogenous.

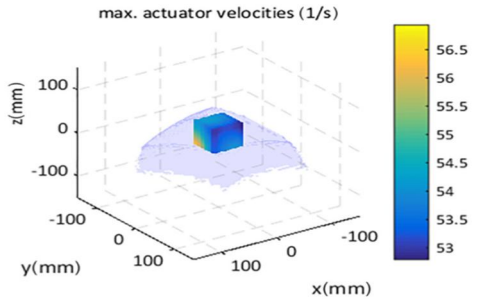

Fig.6. Maximum actuator velocities for each point of the prescribed workspace.

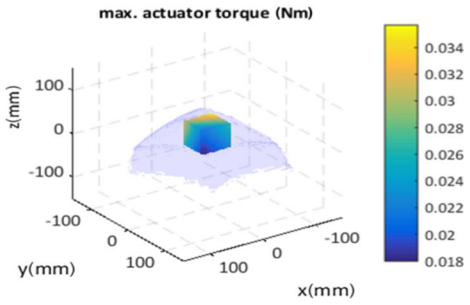

Fig.7. Maximum actuator torque for each point of the prescribed workspace.

One phenomenal element of the introduced robot structure is the auxiliary revolution between each screw and nut, which relies upon the robot present. The sizes of these revolutions are delineated in figures for the base and modified rendition of the robot, individually.

F. Comparison of Base and Modified Version.

The performed examination depends just on the base adaptation, in light of the fact that the distinction of the Jacobian lattices of the base and the modified form is immaterial. Since all the broke down criteria rely upon the Jacobian network, the outcomes for the modified form would be comparable.

IV. JACOBIAN MATRIX.

The converse kinematic calculation is differentiable for both the base and the modified adaptation of the robot. Therefore, the Jacobian grid, defined as J = [∂θ/∂c]T, is found by explanatory separation of the opposite kinematic calculation as defined above.Analytic strategy.

V. CONCLUSION

New methods in radiotherapy, which record for movement of human tissue, will keep on spreading. Such procedures require 4D-apparitions, which imitate previously mentioned movement, along these lines making a similarly spreading new field of utilization of particular robot innovation. In this work, a novel parallel kinematic controller (PKM) has been displayed. Significant focal points of the introduced PKM are:

Simple mechanical arrangement: The PKM can be amassed dependent on for the most part ease standard segments. This empowers a cost bit of leeway of the PKM concerning different robots.

1) *Suitable Smallness:* The elements of the PKM and a human are comparable. This empowers the PKM to be coordinated into a situation which is made for people. For instance, the PKM can be put onto a patient love seat or into a therapeutic imaging gadget. Likewise, the PKM can be moved by hand by the therapeutic faculty.
2) *High Vigor:* A unintentional mechanical effect on the PKM may cause harm of its joints or adjust its kinematic parameters bringing about loss of situating precision. The two circumstances are exceptionally impossible as every one of the connections and joints of the PKM can be effectively intended for high happening powers. Hence, long haul utilization of the PKM in unpleasant states of clinical practice is conceivably conceivable
3) *Spatial Partition of TCP and Actuator Framework:* This is an aftereffect of the extraordinary kinematic structure of the PKM.
4) *Minimal Working Volume of the end-effector inside its Movement Condition:* The end-effector moves in a keyhole design inside the body. This goes along innately with insignificant working volume prerequisite.
5) *Straight-lined access channel to the TCP:* This empowers a simple reconciliation of fastened estimation gadgets into the objective

VI. FUTURE SCOPE

The new type of robot shows better as to the previously mentioned key requests of a 4D-apparition than some other robot utilized so far for this reason. Additionally past the ghost application, the one of a kind qualities of the robot may offer novel benefits, particularly in situations which require execution of complex movement undertakings of the end-effector with insignificant working volume inside a difficult to get to, confined or isolate region. Further work incorporates an inside and out basic burden and firmness investigation and particular streamlining of the basic plan.

REFERENCES

[1] Jinbo Wu and Zhouping Yin (April 1st 2008). A Novel 4-DOF Parallel Manipulator H4, Parallel Manipulators, towards New Applications, Huapeng Wu, Intech Open, DOI: 10.5772/5441. Available from: https://www .intechopen.com/books/parallel_manipulators_towards_new_applications/a_novel_4dof_parallel_manipulator_h4.
[2] A novel four-dimensional radiotherapy method for lung cancer: imaging, treatment planning and delivery H Alasti1,2, Y B Cho, A D Vandermeer, A Abbas, B Norrlinger, S Shubbar and A Bezjak.
[3] The Solid Mechanics of Cancer and Strategies for Improved Therapy, The Solid Mechanics of Cancer and Strategies for Improved Therapy.
[4] Forward Kinematics and Workspace Determination of a Novel Redundantly Actuated Parallel Manipulator Haiqiang Zhang , Hairong Fang , Dan Zhang, Xueling Luo, and Qi Zou.
[5] Effect of Tumour Volume on Drug Delivery in Heterogeneous Vasculature of Human Brain Tumours , Ajay Bhandari, Ankit Bansal, Rishav Jain, Anup Singh, Niraj Sinha1 Department of Mechanical Engineering, Indian Institute of Technology, Kanpur.
[6] Design of a Reconfigurable Quality Assurance Phantom for Verifying the Spatial Accuracy of Radiosurgery Treatments for Multiple Brain Metastases, Journal of Medical Devices. Received November 22, 2018; Accepted manuscript posted August 2, 2019. doi:10.1115/1.4044402 Copyright (c) 2019 by ASME.
[7] A novel four-dimensional radiotherapy method for lung cancer: imaging, treatment planning and delivery H Alasti1,2, Y B Cho1,2, A D Vandermeer1, A Abbas1, B Norrlinger1, S Shubbar3 and A Bezjak2,3.
[8] Telerobotic system concept for real-time soft-tissue imaging during radiotherapy beam delivery ,Jeffrey Schlosser ,Kenneth Salisbury, Dimitre Hristov.

[9] Image-Guided Radiotherapy Using a Modified Industrial Micro-CT for Preclinical Applications.Manuela C. Felix, Jens Fleckenstein,Stefanie Kirschner,Linda Hartmann,Frederik Wenz,Marc A. Brockmann.
[10] Towards MRI guided surgical manipulator. Kiyoyuki Chinzei, Karol Miller Med Sci Monit 2001; 7(1): MT153-163 ID: 421169.
[11] 30 Years of Neurosurgical Robots: Review and Trends for Manipulators and Associated Navigational Systems James Andrew Smith, Jamil Jivraj , Ronnie Wong ,Victor Yang.
[12] Radiotherapy system adapted to monitor a target location in real time. Yu-Jen Chen, Chia-Yuan Liu, Wen-Chung Chang, Chin-Sheng Chen.
[13] On challenges of robot assisted radiotherapy for lung tumours. Lei Ma ; Christian Herrmann ; Klaus Schilling.
[14] Wong J W, Sharpe M B, Jaffray D A, Kini V R, Robertson J M, Stromberg J S and Martinez A A 1999 The use of active breathing control (ABC) to reduce margin for breathing motion Int. J. Radiat. Oncol. Biol. Phys.
[15] Shibamoto Y, Ito M, Sugie C, Ogino H and Hara M 2004 Recovery from sublethal damage during intermittent exposures in cultured tumour cells: implications for dose modification in radiosurgery and IMRT Int. J. Radiat. Oncol. Biol. Phys.
[16] A novel four-dimensional radiotherapy method for lung cancer: imaging, treatment planning and delivery: H Alasti et al 2006 Phys. Med. Biol. 51 3251
[17] Forward Kinematics and Workspace Determination of a Novel Redundantly Actuated Parallel Manipulator. International Journal of Aerospace Engineering Volume 2019, Article ID 4769174, 14 pages https://doi.org/10.1155/2019/4769174
[18] https://www.intechopen.com/books/parallel_manipulators_towards_new_applications/a_novel_4-dof_parallel_manipulator_h4
[19] Four-dimensional image-based treatment planning: Target volume segmentation and dose calculation in the presence of respiratory motion International Journal of Radiation Oncology • Biology • Physics, 61(5), 1535-1550, 2005
[20] https://www.cancer.gov/about-cancer/treatment/types/radiation-therapy
[21] https://www.mayoclinic.org/tests-procedures/radiation-therapy/about/pac-20385162

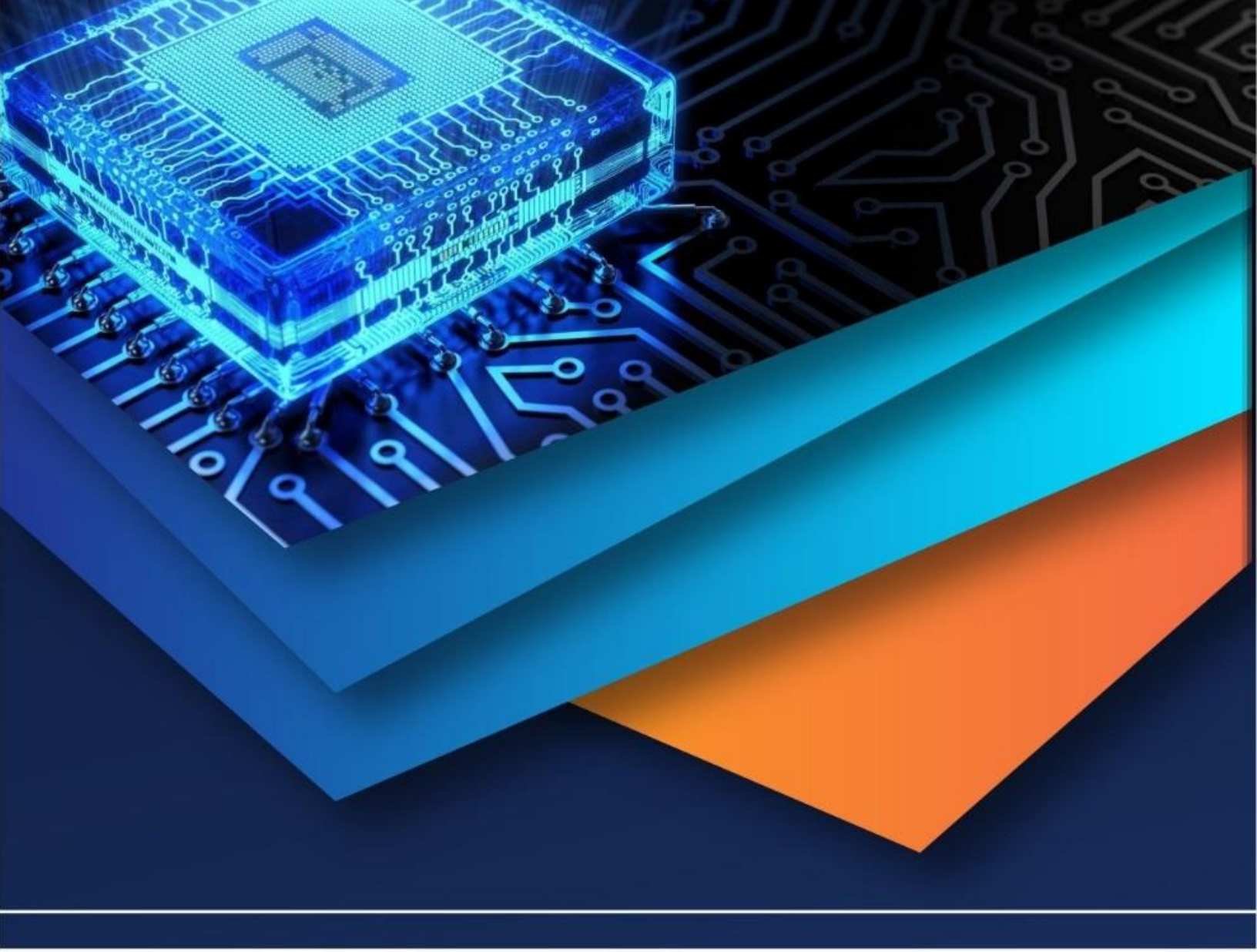

10.22214/IJRASET

45.98

IMPACT FACTOR: 7.129

IMPACT FACTOR: 7.429

INTERNATIONAL JOURNAL FOR RESEARCH

IN APPLIED SCIENCE & ENGINEERING TECHNOLOGY